Available online at www.sciencedirect.com

SciVerse ScienceDirect

Ceramics International 39 (2013) 3435–3439

CERAMICS INTERNATIONAL

www.elsevier.com/locate/ceramint

Short communication

Synthesis of MoO_3 submicron belts and MoO_2 submicron spheres via polyethylene glycol-assisted hydrothermal method and their gas sensing properties

Tayier Yunusi[a], Chao Yang[a], Wanling Cai[a,b], Feng Xiao[a], Jide Wang[a], Xintai Su[a,*]

[a] *Ministry Key Laboratory of Oil and Gas Fine Chemicals, College of Chemistry and Chemical Engineering, Xinjiang University, 14 Shengli Road, Urumqi 830046, China*

[b] *Department of Science, Xinjiang Education Institute, Urumqi, Xinjiang 830043, China*

Received 26 July 2012; received in revised form 24 September 2012; accepted 27 September 2012
Available online 7 October 2012

Abstract

MoO_3 submicron belts and MoO_2 submicron spheres have been synthesized by a polyethylene glycol-assisted hydrothermal method. XRD and SEM images of the products illustrate that MoO_3 submicron belts are about tens of micrometers in length and several hundreds of nanometers in diameter. The products are gradually changed from belt-shaped MoO_3 to spherical MoO_2 with increasing polyethylene glycol as both protective and reducing agent. The products exhibit good responses to acetone and ethanol.

Keywords: A. Powders: chemical preparation; D. Transition metal oxides; E. Sensors; Semiconductors

1. Introduction

Gas sensors based on transition metal oxide semiconductors have been widely used in gas monitoring and emission detection [1,2]. It is well known that the gas sensor properties of the semiconductor gas sensors are influenced not only by the gas sensing materials but also by the morphology and size of the particle [3,4]. Recently, inspired by the superior properties of low dimensional nanomaterials, synthesis of these semiconductor nanoparticles with one-dimensional (1D) or zero-dimensional (0D) microstructures are of current interest [5–8]. However, the works on transitions between zero-dimensional and one-dimensional microstructure are still insufficient. Therefore, it is desired to develop a suitable route to prepare 0D and 1D microstructure materials and investigate their morphology-dependent properties.

Molybdenum oxides mainly include MoO_2 and MoO_3, which have many advanced applications as catalysts, photochromic and electrochromic materials, photo-catalysis, and lithium-ion battery [9–12]. MoO_3, as an n-type semiconductor, has been proven to be a highly sensitive material for the detection of both reducing and oxidizing gases [13,14]. Many works related to the gas sensing properties of MoO_3 have been reported [15,16], however, gas sensors based on MoO_2 have seldom been reported on, and their sensing mechanism remains unclear. A great deal of work has been concerned with the synthesis of molybdenum oxide. Zach et al. developed an electrochemical method for the growth of MoO_3 nanowires on a stepped graphite surface [17]. Traditionally, MoO_2 are made by the reduction of MoO_3 with H_2 at elevated temperatures. Hu and co-workers [18] synthesized MoO_2 nanorods by reduction of MoO_3 nanobelts in an H_2 atmosphere at 550 °C for 1.5 h. Hydrothermal methods involving the reduction of MoO_3 to MoO_2 provide a new approach to synthesis of nano-materials under mild conditions, which offers various morphologies and easy control. To control the shape of final crystals, some assistant agents such as inorganic acid [19], polymers [20] and surfactants [21] were used as structure-directing agent in the hydrothermal or solvent-thermal process. Although there are a lot of successes in the synthesis of molybdenum oxide nanoparticles, it is still indispensable to

*Corresponding author. Tel.: +86 991 8581018; fax: +86 991 8582807.
E-mail address: suxintai827@163.com (X. Su).

0272-8842/$ - see front matter © 2012 Elsevier Ltd and Techna Group S.r.l. All rights reserved.
http://dx.doi.org/10.1016/j.ceramint.2012.09.096

develop a facile and rapid method to prepare MoO_3 and MoO_2 with special morphologies.

In this article, we report the synthesis of MoO_3 submicron belts and MoO_2 submicron spheres by a hydrothermal method using polyethylene glycol (PEG400) as an assistant agent. It is found that the PEG400 plays a vital role in controlling the morphology and phase behavior of the final hydrothermal products. PEG400 is not only acted as a reducing agent and solvent, but also as the structure-directing agent for the formation of MoO_2 submicron spheres. This facile PEG-assisted hydrothermal method provides the opportunity to investigate the transition from 1D to 0D microstructures. The gas sensors based on molybdenum oxide particles show a high response to ethanol and acetone, even at low concentrations and temperatures.

2. Experimental

All the chemical reagents used in the experiment were of analytical grade. The detailed synthesizing process is as follows: 1 g of $(NH_4)_6Mo_7O_{24}\cdot 4H_2O$ was put into 10 ml of deionized water, 10 ml (5 ml or 0 ml) of PEG400 was introduced into the aqueous solution, resulting in a solution. Several milliliters of 3 M HCl was rapidly added under vigorous stirring, giving a transparent sol. After 10 min of stirring, the mixture was transferred into a 100 ml Teflon container, which was filled with distilled water up to 80% of the total volume, sealed and hydrothermally treated at a constant temperature of 180 °C for 48 h. After the reaction completed, the resulting solid products were centrifuged, washed with distilled water and ethanol for more than six times to remove the ions possibly remaining in the final products, and finally dried at 60 °C in air for 60 min.

The obtained samples were characterized by x-ray diffractometer (XRD) using a Rigaku D/max-ga x-ray diffractometer at a scanning of $2^\circ\ min^{-1}$ in 2θ ranging from 10° to 80° with Cu Ka radiation ($\lambda = 1.54178$ Å). The transmission electron microscopy (TEM) analysis was conducted on a model Hitachi H-600 with an accelerating voltage of 100 kV. The scanning electron microscopy (SEM) images were obtained on LEO 1450VP.

Preparation of gas sensors: the gas sensors were prepared by coating a proper paste of MoO_2 or MoO_3 submicrostructrure dispersed with ethanol on alumina ceramic tubes printed with two Au electrodes. After the evaporation of ethanol, the alumina ceramic tubes were coated by a layer of homogeneous MoO_x film. A small Ni–Cr alloy coil was inserted into the tubes as a heater, which was able to provide the working temperature from 80–500 °C for the gas sensors. Before the measurement, the sensors were aged at 300 °C for 3 days to achieve stabilization. The gas sensing measurements were performed in a testing system of WS-30 A (Zhengzhou Winsen Electronics Technology Co. Ltd., PR China).

3. Results and discussion

The overall reaction of the system we used is usually thought to be as follows:

$$(NH4)_6Mo_7O_{24}\ (aq.)+6HCl\ (aq.)\rightarrow 7MoO_3\ (s)+6NH_4Cl\ (aq.)+3H_2O\ (aq.)$$

It is well known that PEG400 can be used as dispersant or protective agent in the hydrothermal system [20,22]. Meanwhile, PEG400 may also act as a reducing agent in the hydrothermal process, which can be confirmed by the following experimental results. The overall reaction can be simplified as follows:

$$MoO_3\ (s)+HOCH_2[CH_2OCH_2]_nCH_2OH\ (aq.)\rightarrow MoO_2\ (s)+HOOC[CH_2OCH_2]_nCOOH\ (aq.)$$

Fig. 1 shows typical XRD patterns of the sample obtained with different volume ratios (absolute PEG400/distilled water, V/V) at 180 °C for 48 h. The XRD image

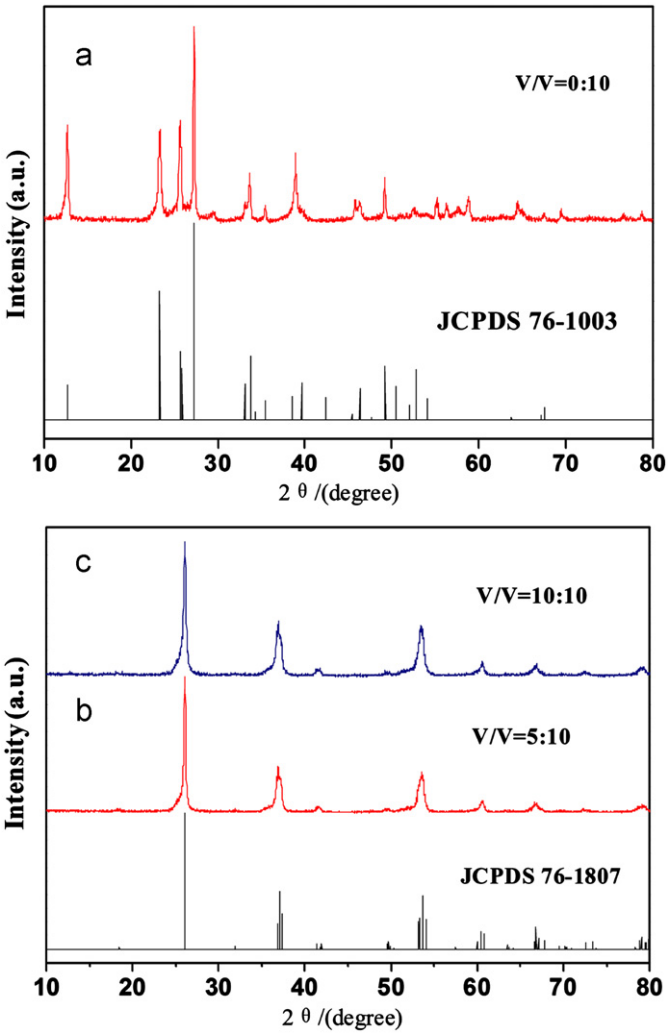

Fig. 1. XRD patterns of the products obtained at 180 °C for 48 h in aqueous solution with different volume ratios (absolute PEG400/distilled water, V/V): (a) 0:10; (b) 5:10 and (c) 10:10.

suggests that in the absence of PEG400, only MoO_3 is obtained, which is consistent with the values in the standard card (JCPDS 76-1003), Fig. 1(a). XRD patterns of the samples prepared in the presence of PEG400 are also given in Fig. 1(b–c); all the reflectance peaks could be indexed to a MoO_2 phase (standard card JCPDS 76-1807), which were suggesting that MoO_3 phase was entirely transformed into MoO_2 phase. No diffractions raised from impurities appear in the XRD patterns, indicating that PEG400 may act as a reducing agent in the system.

The averaged crystallite sizes D were determined from the XRD pattern according to the Scherrer equation $D=k\lambda/\beta\cos\theta$, where k is a constant (shape factor, about 0.9), λ is the x-ray wavelength (0.15418 nm), β is the full width at half maximum (FWHM) of diffraction line, and θ is the diffraction angle. The calculated crystallite sizes of powders (from (a) to (c)) were 36, 28 and 23 nm, respectively. This suggested that the crystallite sizes decreased with the increase of PEG400.

Typical SEM images which confirm that PEG400 can work as a protective agent are shown in Fig. 2. When PEG400 is not used, belt-shaped products were obtained (Fig. 2(a)). The products have uniform belt-morphologies with diameters of 200–300 nm and lengths up to several micrometers. When PEG400 (absolute PEG400/distilled water, V/V, 5:10) was introduced to the hydrothermal system, spherical particles products (Fig. 2(b)) were produced besides belt-shaped products. The diameters of the spherical particles were in the range of 1–3 μm. The higher magnification SEM observation (shown in the inset graph) indicates that those spheres are aggregated from smaller nanoparticles. When the volume ratio of PEG400 to distilled water was increased to 10:10, homogenous submicron spheres were obtained, with diameters ranging from 100 to 150 nm (Fig. 2 (c)).

The obtained MoO_x products are further characterized by TEM. Fig. 3(a) shows the TEM image of typical belt-shaped MoO_3 nanostructures which is in consistence with the SEM observation. The belt-shaped MoO_3 particles overlap on each other, forming relatively wide belts with width of about 200–300 nm. However, when 5 ml of PEG400 is added to the reaction system, submicro-sized or micro-sized spherical particles are produced besides belt-shaped products (Fig. 2(b)). With the increase of PEG400 added to the solution, all of the belt-shaped particles disappear and only highly uniform submicro-sized spherical particles are obtained (Fig. 3(c)). Of particular interests, the MoO_2 submicron spheres under the radiation of electrons are also be composed of many particles with sizes of about 20–40 nm, indicating that such submicron-scale sphere is aggregated from nanoparticles. Such kind of self-assemblies of nanoparticles is probably due to the decrease of surface energy of the system. TEM and SEM images suggest that the ratio of PEG400 to distilled water in the initial solution plays a significant role in determining the final morphologies of MoO_x particles.

The finely homogeneous and well-crystallized particles with regular spherical morphologies are probably formed through a mechanism similar to those proposed for the formation of $La(OH)_3$ or $WO_3\cdot 2H_2O$ nanocrystals [23,24]. According to this mechanism, PEG400 plays the role of a structure-directing agent to control the growth rate of

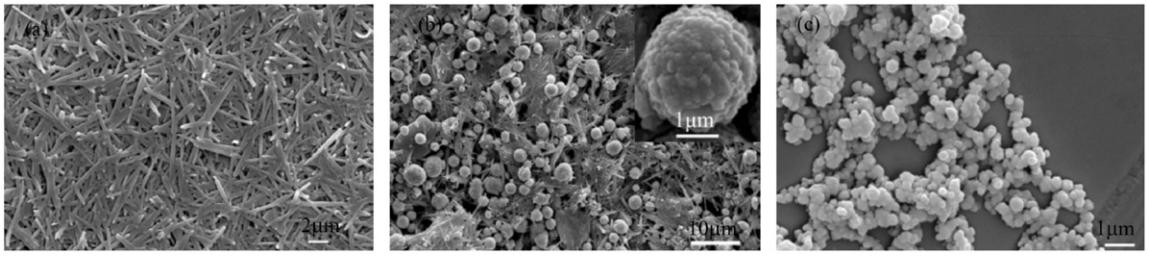

Fig. 2. SEM images of the samples prepared at 180 °C for 48 h in aqueous solution with different volume ratios (absolute PEG400/distilled water, V/V): (a) 0:10; (b) 5:10; and (c) 10:10.

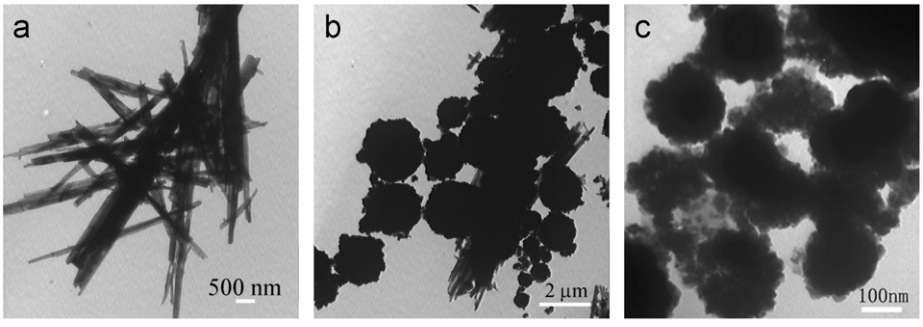

Fig. 3. TEM images of the samples prepared at 180 °C for 48 h in aqueous solution with varied volume ratios (absolute PEG400/distilled water, V/V): (a) 0:10; (b) 5:10 and (c) 10:10.

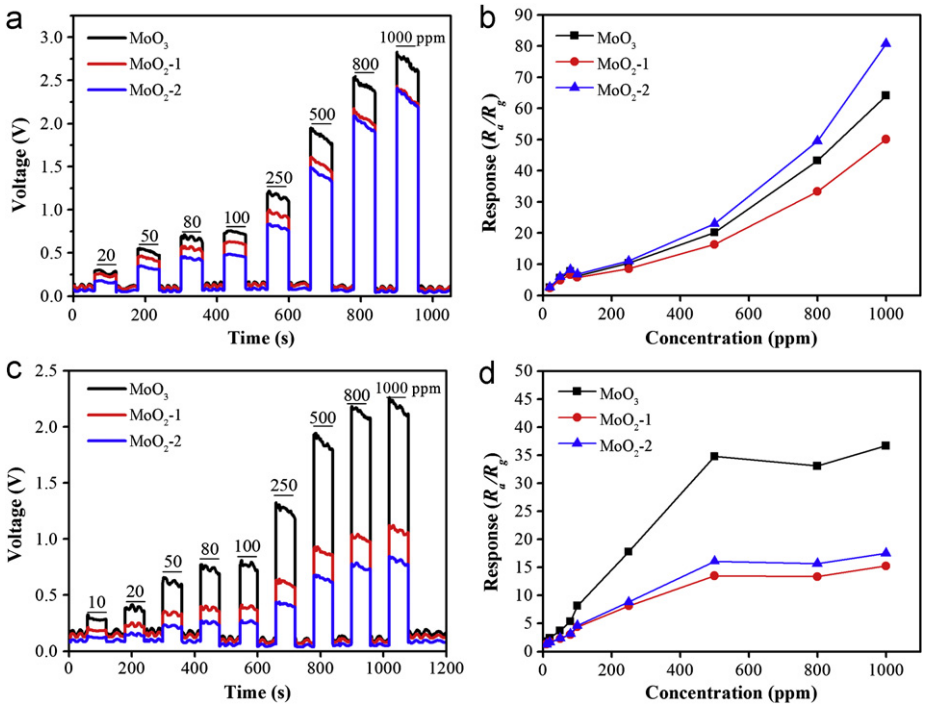

Fig. 4. Real-time gas responses to (a) ethanol and (c) acetone of the sensors fabricated from belt-like MoO_3 a mixture of MoO_2 submicron belts and submicron spheres (MoO_2-1) and spherical MoO_2 (MoO_2-2) at operating temperature of 370 °C. Sensing response of the sensors to (b) ethanol and (d) acetone as a function of gas concentration.

nanoparticles in different directions. Molybdenum oxide is an anisotropic material, and one-dimensional belt-shaped products are easily obtained under hydrothermal conditions. PEG400 can be adsorbed on the surface of the crystallites, forming a protective layer to hold back the growth rate of molybdenum oxide particles. Meanwhile, PEG400 may act as a reduction agent in the hydrothermal process. With the increase of PEG400, the structure-directing effect of PEG400 becomes more obvious, and the products change from belt-shaped MoO_3 to spherical MoO_2.

The gas sensing performance of the as-obtained MoO_x-based products is investigated using ethanol and acetone as the model gases as shown in Fig. 4. Fig. 4(a) shows typical isothermal response curves of MoO_3- and MoO_2-based sensors to ethanol vapor with concentrations from 20 to 1000 ppm in ambient air. It can be seen that the resistance of the sensors immediately increases upon exposure to ethanol, and reversely drops to the initial values in air. After repeated switches between the test gas and air, the resistance still decreases to the original state, indicating that the sensors have good repeatability and reversibility. The sensors response is defined as the ratio of R_a to R_g (R_a/R_g), in which R_a is the resistance in air and R_g is the resistance in the gas. The ethanol sensing response (Fig. 4(b)) shows a step increase for all the three sensors with increasing the ethanol concentration. Among them, the spherical MoO_2-based sensor shows the highest response of 80.8 to 1000-ppm ethanol compared to that of 64.1 for belt-like MoO_3 and that of 50.1 for the mixture of MoO_2 submicron belts and submicron spheres. Fig. 4(c) shows dynamic sensing curves of the sensors to acetone at 370 °C. The sensor based on belt-like MoO_3 exhibits significant sensing magnitudes over the other two sensors. Correspondingly, the acetone response (Fig. 4(d)) of the belt-like MoO_3 is 36.7 at a concentration of 1000 ppm, which is higher than that of 17.5 for spherical MoO_2 and that of 15.2 for the mixture of MoO_2 submicron belts and submicron spheres. Moreover, this result indicates that belt-like MoO_3 shows more sensitive to acetone than spherical MoO_2, although the latter has higher responses to ethanol than the former. These selective responses to different gases provide an opportunity for the fabrication of MoO_x-based sensors with high selectivity.

4. Summary

In summary, a simple hydrothermal method was used to prepare MoO_3 submicron belts and MoO_2 submicron spheres. The shape and phase of the MoO_x-based products can be controlled with the aid of PEG400. This work may explore a possible direction to synthesize spherical products in the solution-based approach. The gas sensing results show that the MoO_3 and MoO_2 crystallites have a high sensor response to acetone and ethanol, respectively. It is sensitive to ethanol and acetone at low temperature, thus presenting very important features for practical use.

Acknowledgments

This work was supported by NSFC (21163020), the Key Project of Chinese Ministry of Education (211199) and the Natural Science Foundation of Xinjiang Province (2011211A021).

References

[1] Y. Wang, X. Jiang, Y. Xia, A solution-phase, precursor route to polycrystalline SnO_2 nanowires that can be used for gas sensing under ambient conditions, Journal of the American Chemical Society 125 (52) (2003) 16176–16177.

[2] N. Pinna, G. Neri, M. Antonietti, M. Niederberger, Nonaqueous synthesis of nanocrystalline semiconducting metal oxides for gas sensing, Angewandte Chemie International Edition 43 (33) (2004) 4345–4349.

[3] S. Pokhrel, C.E. Simion, V.S. Teodorescu, N. Barsan, U. Weimar, Synthesis, mechanism, and gas-sensing application of surfactant tailored tungsten oxide nanostructures, Advanced Functional Materials 19 (11) (2009) 1767–1774.

[4] X. Han, M. Jin, S. Xie, Q. Kuang, Z. Jiang, Y. Jiang, Z. Xie, L. Zheng, Synthesis of tin dioxide octahedral nanoparticles with exposed high-energy {221} facets and enhanced gas-sensing properties, Angewandte Chemie International Edition 48 (48) (2009) 9180–9183.

[5] Z. Tang, N.A. Kotov, One-dimensional assemblies of nanoparticles: preparation, properties, and promise, Advanced Materials 17 (8) (2005) 951–962.

[6] Y. Xia, T.D. Nguyen, M. Yang, B. Lee, A. Santos, P. Podsiadlo, Z. Tang, S.C. Glotzer, N.A. Kotov, Self-assembly of self-limiting monodisperse supraparticles from polydisperse nanoparticles, Nature Nanotechnology 6 (2011) 580–587.

[7] Y. Xia, Z. Tang, Monodisperse hollow supraparticles via selective oxidation, Advanced Functional Materials 22 (2012) 2585–2593.

[8] Y. Xia, Z. Tang, Monodisperse inorganic supraparticles: formation mechanism, properties and applications, Chemical Communications 48 (2012) 6320–6336.

[9] M. Shokouhimehr, Y. Piao, J. Kim, Y. Jang, T. Hyeon, A magnetically recyclable nanocomposite catalyst for olefin epoxidation, Angewandte Chemie International Edition 119 (37) (2007) 7169–7173.

[10] L. Zheng, Y. Xu, D. Jin, Y. Xie, Novel metastable hexagonal MoO_3 nanobelts: synthesis, photochromic, and electrochromic properties, Chemical Materials 21 (23) (2009) 5681–5690.

[11] L.X. Song, J. Xia, Z. Dang, J. Yang, L.B. Wang, J. Chen, Formation, structure and physical properties of a series of α-MoO_3 nanocrystals: from 3D to 1D and 2D, CrystEngComm 14 (8) (2012) 2675–2682.

[12] T. Brezesinski, J. Wang, S.H. Tolbert, B. Dunn, Ordered mesoporous α-MoO_3 with iso-oriented nanocrystalline walls for thin-film pseudocapacitors, Nature Materials 9 (2) (2010) 146–151.

[13] A.M. Azad, Fine-tuning of ceramic-based chemical sensors via novel microstructural modification—part II: low level CO sensing by molybdenum oxide, MoO_3, Sensors and Actuators B 120 (1) (2006) 25–34.

[14] S. Barazzouk, R.P. Tandon, S. Hotchandani, MoO_3-based sensor for NO, NO_2 and CH_4 detection, Sensors and Actuators B 119 (2) (2006) 691–694.

[15] W.S. Kim, H.C. Kim, S.H. Hong, Gas sensing properties of MoO_3 nanoparticles synthesized by solvothermal method, Journal of Nanoparticle Research 12 (5) (2010) 1889–1896.

[16] D.L. Chen, M.N. Liu, L. Yin, T. Li, Z. Yang, X.J. Li, B.B. Fan, H.L. Wang, R. Zhang, Z.X. Li, H.L. Xu, H.X. Lu, D.Y. Yang, J. Sun, L. Gao, Single-crystalline MoO_3 nanoplates: topochemical synthesis and enhanced ethanol-sensing performance, Journal of Materials Chemistry 21 (25) (2011) 9332–9342.

[17] M.P. Zach, K. Inazu, K.H. Ng, J.C. Hemminger, R.M. Penner, Synthesis of molybdenum nanowires with millimeter-scale lengths using electrochemical step edge decoration, Chemistry of Materials 14 (7) (2002) 3206–3216.

[18] B. Hu, L. Mai, W. Chen, F. Yang, From MoO_3 nanobelts to MoO_2 nanorods: structure transformation and electrical transport, ACS Nano 3 (2) (2009) 478–482.

[19] M. Yan, Y. Shen, L. Zhao, Z. Li, Synthesis and photochromic properties of EDTA-induced MoO_3 powder, Materials Research Bulletin 46 (10) (2011) 1648–1653.

[20] C.V. Subba Reddy, E.H. Walker Jr, C. Wen, S. i. Mho, Hydrothermal synthesis of MoO_3 nanobelts utilizing poly(ethylene glycol), Journal of Power Sources 183 (1) (2008) 330–333.

[21] S. Hu, X. Wang, Single-walled MoO_3 nanotubes, Journal of the American Chemical Society 130 (26) (2008) 8126–8127.

[22] Z. Wang, H. Wang, C. Yang, J. Wu, Synthesis of molybdenum oxide hollow microspheres by ethanol and PEG assisting hydrothermal process, Materials Letters 64 (20) (2010) 2170–2172.

[23] B. Tang, J.C. Ge, L.H. Zhuo, The fabrication of $La(OH)_3$ nanospheres by a controllable-hydrothermal method with citric acid as a protective agent, Nanotechnology 15 (12) (2004) 1749.

[24] Q. Sun, J. Luo, Z. Xie, J. Wang, X. Su, Synthesis of monodisperse $WO_3 \cdot 2H_2O$ nanospheres by microwave hydrothermal process with L (+) tartaric acid as a protective agent, Materials Letters 62 (17–18) (2008) 2992–2994.